Published in final edited form as:
Cell. 2012 March 30; 149(1): 173–187. doi:10.1016/j.cell.2011.12.038.

Wnt Signaling Regulates Acetylcholine Receptor Translocation and Synaptic Plasticity in the Adult Nervous System

Michael Jensen, **Frédéric J. Hoerndli**, **Penelope J. Brockie**, **Rui Wang**, **Erica Johnson**, **Dane Maxfield**, **Michael M. Francis**[†], **David M. Madsen**, and **Andres V. Maricq**[*]
Department of Biology University of Utah Salt Lake City, UT 84112-0840

Summary

The adult nervous system is plastic allowing us to learn, remember and forget. Experience-dependent plasticity occurs at synapses – the specialized points of contact between neurons where signaling occurs. However, the mechanisms that regulate the strength of synaptic signaling are not well understood. Here, we define a Wnt signaling pathway that modifies synaptic strength in the adult nervous system by regulating the translocation of one class of acetylcholine receptors (AChRs) to synapses. In *C. elegans*, we show that mutations in CWN-2 (Wnt ligand), LIN-17 (Frizzled), CAM-1 (Ror receptor tyrosine kinase), or the downstream effector DSH-1 (disheveled) result in similar subsynaptic accumulations of ACR-16/α7 AChRs, a consequent reduction in synaptic current, and predictable behavioral defects. Photoconversion experiments revealed defective translocation of ACR-16/α7 to synapses in Wnt signaling mutants. Using optogenetic nerve stimulation, we demonstrate activity-dependent synaptic plasticity and its dependence on ACR-16/α7 translocation mediated by Wnt signaling via LIN-17/CAM-1 heteromeric receptors.

Introduction

Central to information processing by neural networks is neurotransmitter-mediated communication between neurons at specialized points of contact called synapses. Here, neurotransmitter is released at the presynaptic membrane and binds to neurotransmitter receptors specifically localized in the postsynaptic membrane apposed to presynaptic release sites (Jin and Garner, 2008). Synapses are dynamic structures in the adult nervous system and individual synapses undergo activity-dependent plasticity that is believed to underlie learning and memory (Kessels and Malinow, 2009).

In part, synaptic plasticity depends on the insertion and removal of specific neurotransmitter receptors, thus strengthening or weakening the synapse. A common strategy for changing the number of membrane proteins is to shuttle proteins between intracellular pools and the cell surface (Kennedy and Ehlers, 2011). This strategy is used for diverse homeostatic processes, including synaptic plasticity (Turrigiano, 2008), aquaporin-mediated fluid homeostasis (Brown et al., 2009), and insulin-induced translocation of glucose transporters (Watson and Pessin, 2007). Yet for all of these receptor pathways, we still have only a limited understanding of how trafficking from cytoplasmic compartments to the membrane

[*]Corresponding author (maricq@biology.utah.edu).
[†]Current address: Department of Neurobiology, University of Massachusetts, Worcester, MA

is regulated. To gain a comprehensive mechanistic understanding of this process at synapses, we used a genetic approach in *C. elegans* to identify and study the signaling molecules that regulate neurotransmission at a model synapse.

The *C. elegans* neuromuscular junction (NMJ) has features usually associated with neuronal synapses, such as multiple classes of neurotransmitter receptors and excitatory cholinergic (ACh) and inhibitory GABAergic synaptic inputs. Synaptic release from cholinergic neurons depolarizes the postsynaptic membrane by activating two independent classes of AChRs that are defined by both pharmacological and genetic criteria. We previously found that CAM-1, a Ror-family receptor tyrosine kinase (RTK), is selectively required for signaling mediated by one of these receptor classes, ACR-16, which is the *C. elegans* homolog of the vertebrate α7 AChR (Francis et al., 2005). In *cam-1* mutants, the decreased ACh-gated current appears to be secondary to reduced surface delivery of ACR-16/α7. We found that ACR-16/α7 localization and ACR-16/α7-mediated currents were rescued in transgenic *cam-1* mutants that expressed a CAM-1 variant that included the extracellular and transmembrane domains, but lacked the intracellular kinase domain (Francis et al., 2005). These results suggested that CAM-1 might contribute to a cell-surface receptor that regulates the synaptic delivery of ACR-16/α7. Interestingly, the extracellular domain of CAM-1 contains a cysteine-rich (CR) domain predicted to bind to small, secreted glycoproteins called Wnts.

Receptor tyrosine kinases (RTKs), Wnts and Frizzled proteins (Wnt receptors) have diverse roles in the development of the nervous system, including cell migration, cell polarity and axon outgrowth (Budnik and Salinas, 2011; Green et al., 2008; Kennerdell et al., 2009; van Amerongen and Nusse, 2009). Furthermore, Wnts have conserved roles at developing synapses in flies, worms and vertebrates (Budnik and Salinas, 2011; Farias et al., 2010; Korkut and Budnik, 2009). For example, elegant genetic studies in *Drosophila* larva have demonstrated that Wnt signaling can modify the structure and function of developing glutamatergic synapses (Ataman et al., 2008; Korkut et al., 2009).

In mammals, Wnts interact with the muscle specific kinase (MuSK) at the NMJ to coordinate AChR aggregation and motor neuron growth cone targeting (Henriquez et al., 2008; Wu et al., 2010). At neuronal synapses, Wnt7a induces presynaptic clustering of α7 AChRs with adenomatous polyposis coli (APC) in rat hippocampal neurons, directs synapse formation in the mouse brain (Farias et al., 2007; Hall et al., 2000; Sahores et al., 2010), and regulates the number and strength of hippocampal synapses (Ciani et al., 2011). Application of exogenous Wnts has diverse effects on neuronal structure and synaptic communication, including pre- and post-synaptic differentiation, spine density, receptor endocytosis and recycling (Cuitino et al., 2010; Inestrosa and Arenas, 2010).

Despite our detailed knowledge of Wnt signaling during development, we know far less about Wnt regulation of synaptic signaling, and whether this regulation continues in the mature nervous system. To address these questions, we have taken advantage of the strengths of *C. elegans* for the study of synaptic signaling. The *C. elegans* genome is predicted to encode conserved members of the Wnt signaling pathway, and there are available mutants for the five Wnt ligands, four Fzd receptors, three Dvl proteins, one Ryk/*derailed* receptor, and one Ror RTK (www.wormbase.org).

In this study, we present evidence that Wnt signaling, mediated through a heteromeric Ror/Fzd receptor complex, has an ongoing and important role in shaping transmission at mature synapses in adult animals. We found that mutations in LIN-17 (Fzd), CWN-2 (Wnt), or DSH-1 (Dvl) phenocopied the movement, electrophysiological, and ACR-16/α7 localization defects observed in *cam-1* mutants (Francis et al., 2005). Importantly, expression of LIN-17/Fzd driven by a heat shock promoter at the adult stage rescued the ACR-16/α7-dependent

behavior of *lin-17* mutants, indicating that Wnt signaling has a persistent role in synaptic transmission. Using a new paradigm for plasticity, we also found that optogenetic stimulation of motor neurons induced activity dependent changes in ACR-16/α7 localization and current, and that these changes were abolished in Wnt-signaling mutants. CWN-2 signaling by motor neurons was both necessary and sufficient for rescue of these activity-dependent changes in *cwn-2* mutants. In confirmation of this model, we found that application of recombinant CWN-2 rapidly increased ACR-16/α7-mediated current. In summary, our studies have identified a Wnt signaling pathway that controls the translocation of ACR-16/α7 receptors to synapses, and has a critical role in modulating the strength of established synapses in the adult nervous system.

Results

Wnt signaling contributes to ACR-16/α7-mediated current and behavior

In *C. elegans*, two classes of acetylcholine-gated ion channels – levamisole sensitive (L-AChR) and nicotine sensitive (N-AChR) – and one class of GABA-gated ion channels are expressed in muscle cells (Figure 1A) and are necessary for normal worm movement (de Bono and Maricq, 2005; Francis et al., 2005). L-AChRs are ionotropic transmembrane proteins composed of various pentameric combinations of the AChR subunits UNC-38, UNC-63, LEV-1, LEV-8 and UNC-29 (Boulin et al., 2008). In contrast, N-AChRs are homopentamers of the ACR-16 subunit, which is similar to the neuronal type α7 nicotinic AChR in vertebrates (Francis et al., 2005; Touroutine et al., 2005). The CAM-1/Ror RTK is also expressed in muscle cells (Francis et al., 2005), and in *cam-1* mutants the ACh-gated currents mediated by ACR-16/α7 are reduced compared to those measured in wild-type muscle cells (Figure 1B and C). Additionally, in *cam-1* mutants ACR-16/α7 receptors abnormally accumulate in postsynaptic muscle arms – projections that extend from muscles to neurons in the ventral nerve cord. However, ACh-gated currents mediated by L-AChRs and GABA-gated currents are not appreciably affected in *cam-1* mutants (Francis et al., 2005).

The majority of ACh-gated current at the NMJ is dependent on ACR-16/α7; but surprisingly, *acr-16* mutants do not have a discernable defect in locomotion when on standard assay plates (Francis et al., 2005; Touroutine et al., 2005). However, when we challenged *acr-16* mutants with a more rigid substrate (see Experimental Procedures), we found that their movement was diminished compared to wild-type controls, and this defect could be rescued by muscle specific expression of ACR-16/α7 (Figure S1A).

The reduced ACh-gated current in *cam-1* mutants can be rescued by expressing a truncated variant of CAM-1 lacking the intracellular tyrosine kinase domain, CAM-1(ΔTKD), under control of the native *cam-1* promoter (Francis et al., 2005). To further delimit the site of action, we found that muscle-specific expression of GFP tagged CAM-1(ΔTKD), but not neuronal expression, was sufficient to rescue ACR-16/α7-mediated currents (Figure 1B and C). These results suggest that changes in ACR-16/α7-mediated signaling might depend on interactions between the extracellular domain of CAM-1 and other signaling molecules at the muscle membrane. We tested this hypothesis by expressing a muscle-specific GFP-tagged variant of CAM-1 that lacked the extracellular domain, CAM-1(ΔECD)::GFP, and found that it was not sufficient to rescue ACh-gated current in *cam-1* mutants (Figure 1B and C).

The dependence of CAM-1 function on the ECD, but not the TKD, led us to search for gene products that might interact with CAM-1 and contribute to the regulation of synaptic ACR-16/α7 receptors. In heterologous cells, Ror RTKs have been shown to bind frizzled (Fzd) receptors, which are seven-pass transmembrane proteins required for Wnt-mediated

signaling (Oishi et al., 2003). Because the intracellular kinase domain of CAM-1 is not required for ACR-16/α7-mediated current, CAM-1 might function via a kinase-independent mechanism – possibly by interacting with a Fzd receptor (Francis et al., 2005; Zinovyeva et al., 2008).

We took advantage of our earlier observation that *unc-29; acr-16* double mutants have a synthetic, near-paralyzed phenotype (Francis et al., 2005), and reasoned that if Wnt-signaling was required for ACR-16/α7-mediated currents then mutations in genes predicted to contribute to Wnt-signaling should also have a synthetic phenotype with the *unc-29* mutation (gene alleles described in Table S1). We therefore made double mutants with *unc-29* and candidate Wnt-signaling mutants and tested these in a movement assay (thrashing in liquid). We found that mutations in a Wnt ligand (CWN-2), a Frizzled receptor (LIN-17), and an intracellular signaling molecule Dishevelled (DSH-1) all had synthetic movement defects similar to those observed in *unc-29; acr-16* and *unc-29; cam-1* double mutants (Figure 1D); but the single mutants were not nearly as impaired (Figure S1B). We also found that locomotion on agar plates was disrupted in *unc-29; lin-17* double mutants and that this defect was rescued by muscle-specific expression of LIN-17 (Figure S1C). We did not observe comparable defects in the Frizzled mutants *mig-1* and *cfz-2*, the Wnt mutants *cwn-1* and *egl-20*, or the Ryk/Derailed mutant *lin-18* (Figure 1D and data not shown). This indicates that only a subset of known Wnt-signaling proteins function in this synaptic signaling pathway.

We next asked whether the Wnt signaling pathway was dependent on CWN-2, or if other Wnt ligands could substitute for CWN-2. However, we found no evidence that thrashing behavior was rescued in transgenic *unc-29*; *cwn-2* mutants that expressed the Wnts EGL-20 or LIN-44 driven by the *cwn-2* promoter (Figure S1D).

ACR-16/α7-mediated currents are selectively diminished in Wnt signaling mutants

To directly test whether Wnt signaling is required for normal synaptic function, we used standard electrophysiological techniques to record *in vivo* currents in muscle evoked by pressure application of ACh. We found that the magnitude of the ACh-gated current was significantly diminished for each of the Wnt-signaling mutants (Figure 1E and F). The reduced current appeared to be secondary to a selective decrease in the fast, ACR-16/α7-mediated component of the ACh-gated current, similar to what was observed for *cam-1* and *acr-16* mutants. This was confirmed by the observed reduction in nicotine-gated currents in *cwn-2* and *lin-17* mutants (Figure S2A). Furthermore, ACh-gated currents in *lin-17; cam-1* double mutants were indistinguishable from either single mutant alone, suggesting that CAM-1 and LIN-17 function in the same signaling pathway (Figure 1E and F).

The slow component of the current is mediated by UNC-29-containing ionotropic receptors that are selectively activated by levamisole (Francis et al., 2005; Richmond and Jorgensen, 1999). We therefore measured levamisole-gated currents in Wnt-signaling mutants to determine whether these mutations disrupt the UNC-29-mediated component of the ACh-gated current. We found that levamisole-gated currents in these mutants were indistinguishable from wild type (Figure S2B), suggesting that Wnt-signaling is specifically required for ACR-16/α7-mediated current. As an additional control, we found that GABA-activated currents were normal in *cwn-2* mutants (Figure S3A). ACh-gated currents were not disrupted in *cwn-1*, *lin-44* or *egl-20* mutants, providing further evidence for specificity of CWN-2 signaling (Figure S3B). Together, our results indicate that Wnt signaling is required for ACR-16/α7-mediated whole-cell currents.

Presynaptic release is not appreciably disrupted in Wnt signaling mutants

To further evaluate synaptic transmission, we measured endogenous cholinergic synaptic activity. We found a similar decrease in the average amplitude of the miniature excitatory postsynaptic current (mEPSC) for each of the Wnt signaling mutants (Figure S3C). In contrast, we did not observe a significant change in mEPSC frequency (wild type, 25 ± 4/s; *cam-1*, 20 ± 7/s; *cwn-2*, 20 ± 5/s; *lin-17*, 23 ± 12/s; and *dsh-1,* 14 ± 8/s, $p>0.05$), indicating that endogenous presynaptic release was not obviously disrupted in the Wnt signaling mutants.

We also asked whether Wnt signaling contributed to nerve-evoked current. To measure these currents, we expressed the light-gated ion channel channelrhodopsin-2 (ChR2) in cholinergic motor neurons and used light to depolarize these motor neurons (Liewald et al., 2008; Liu et al., 2009). We found that light stimulation elicited reproducible nerve-evoked postsynaptic currents in both wild type and *cwn-2* mutants (Figure S2C). However, the peak amplitude of nerve-evoked current was significantly reduced in *cwn-2* mutants while the steady state current, which reflects the contribution of levamisole receptors, was not significantly altered. These results are consistent with the decreased amplitude of mEPSCs (Figure S3C) and the reduction in ACh-gated current (Figure 1E and F).

Neuronal Wnt acts through muscle expressed Fzd/Ror/Dvl to regulate ACR-16/α7-mediated behavior and current

The Wnt signaling proteins identified in our screen are expressed in muscles and neurons (Gleason et al., 2006) raising the question of whether these proteins are required in a specific tissue for ACR-16/α7-mediated behavior and current. To address this question, we first examined whether the *cwn-2* mutants could be rescued by selective expression of the wild-type protein in either muscles or neurons. To isolate the ACR-16/α7-mediated behavior and current, we measured thrashing behavior and recorded ACh-evoked currents in the *unc-29* mutant background. Interestingly, we found that thrashing in *cwn-2* mutants was rescued by expressing wild-type CWN-2, a secreted protein, in neurons or muscles (Figure 2A).

Although this finding for sufficiency is consistent with CWN-2's role as a secreted signaling molecule in other tissues (Kennerdell et al., 2009), we sought to address the question of necessity by using RNAi to selectively knock down expression of *cwn-2* in muscles or neurons. Successful knock down was indicated by an RNAi-mediated decrease in secreted CWN-2::mCherry fluorescence (Figure S3D). We found that knock down in neurons, but not in muscles, phenocopied both the synthetic thrashing and current defects observed in *unc-29;cwn-2* mutants (Figure 2B–D).

We next asked whether DSH-1 and LIN-17 are required in muscles or neurons. We found that both thrashing and current defects of *lin-17* and *dsh-1* mutants were rescued by selectively expressing wild-type transgenes in muscles. In contrast, we did not observe rescue with neuron-specific expression (Figure 2E–J). These results are also consistent with our finding that CAM-1(ΔTKD)::GFP expression in muscle cells rescued current defects in the muscles of *cam-1* mutants (Figure 1B and C).

CAM-1 and LIN-17 function in the same pathway to regulate ACR-16/α7 at synapses

Our analysis of single mutants revealed that the behavioral and electrophysiological phenotypes of Wnt-signaling mutants were similar to those of *cam-1* mutants. Additional genetic analysis revealed that ACh-gated currents recorded from *lin-17; cam-1* double mutants were of similar magnitude and kinetics to those recorded from *cam-1* and *lin-17* single mutants (Figure 1E and F). These data suggested that the LIN-17 frizzled receptor and the CAM-1 RTK function in the same pathway. Because the extracellular domain (ECD) of

CAM-1 is required for its function at synapses, we speculated that CAM-1 and LIN-17 might interact directly via the ECDs of each protein, possibly forming a heteromeric receptor. To further test this possibility, we examined the subcellular localization of LIN-17 and CAM-1. We found that these functional, fluorescently labeled proteins were expressed in muscle arms of transgenic worms and partially co-localized (Figure 3A) suggesting that LIN-17 and CAM-1 might associate in muscle arms.

To address this possibility, we tested bimolecular fluorescence complementation (BiFC) between LIN-17 and CAM-1 (Shyu et al., 2008). We used a split variant of the Venus Yellow Fluorescent Protein (YFP) and fused the N- and C-terminal fragments of Venus YFP to the intracellular regions of CAM-1(CAM-1::N-YFP) and LIN-17 (LIN-17::C-YFP), respectively. We observed distinct YFP puncta in the muscle arms abutting the ventral cord in transgenic worms that co-expressed the LIN-17::C-YFP and CAM-1::N-YFP fusion proteins (Figure 3B). Transgenic worms that expressed either the N- or C-terminal YFP fragment alone exhibited no fluorescence, but we observed a punctate YFP signal in cross progeny that expressed both transgenes (Figure S4A).

The CAM-1 ECD is predicted to be important for Wnt binding and perhaps for interactions between the receptor components (Green et al., 2007; Kim and Forrester, 2003). To determine whether the ECD was required for the interaction between CAM-1 and LIN-17, we generated a split-YFP-tagged CAM-1 variant that lacked the ECD (CAM-1(ΔECD)::N-YFP) and as a control a tagged variant that lacked the intracellular kinase domain (CAM-1(ΔTKD)::N-YFP). We found YFP puncta in transgenic worms that co-expressed CAM-1(ΔTKD)::N-YFP and LIN-17::C-YFP in muscles (Figure 3C), but no appreciable fluorescent signal in worms that co-expressed CAM-1(ΔECD)::N-YFP and LIN-17::C-YFP (Figure 3D). These data suggest that the CAM-1 ECD is required for the association of LIN-17 with CAM-1, and that the fluorescent signal is not simply due to overexpression of the tagged proteins. Although the ECD was required for BiFC fluorescence, examination of GFP-labeled CAM-1(ΔECD) indicated that this domain was not essential for CAM-1 expression at the NMJ (Figure 3E).

Our finding that the CAM-1 ECD mediates its interaction with LIN-17 is consistent with our earlier finding that CAM-1(ΔTKD) rescues current when expressed in transgenic *cam-1* mutants (Francis et al., 2005) (Figure 1B and C). Together, these results provide evidence for a mechanistic model in which CAM-1 and LIN-17 form a functional heteromeric receptor in muscle cells. This model is also consistent with our analysis of *lin-17; cam-1* double mutants (Figure 1E and F), which showed that LIN-17 and CAM-1 function in the same signaling pathway to regulate ACR-16/α7-mediated current.

Postsynaptic ACR-16/α7 receptors are mislocalized in Wnt signaling mutants

ACR-16::GFP fluorescence is found at the tips of muscle arms apposed to presynaptic release sites in the cholinergic motor neurons traveling in the ventral cord (Figure 3F and G). In *cam-1* mutants, we previously observed subsynaptic accumulations of ACR-16::GFP in muscle arms, but no change in the distribution of UNC-49::GFP GABA receptors or UNC-29::GFP L-AChRs (Francis et al., 2005). We found that ACR-16::GFP was similarly mislocalized in other Wnt signaling mutants (Figure 3H). Whereas the distribution of ACR-16 was markedly altered in *cwn-2* mutants, the distribution of the SYD-2 presynaptic protein did not appear appreciably altered (Figure 3G). Furthermore, we did not detect obvious changes with respect to the morphology of body wall muscles or the number of muscle arms (Figure S4B).

For each Wnt signaling mutant, the average intensity of ACR-16::GFP was dramatically increased in the muscle arms (Figure 3I). The defects were rescued in *lin-17* and *dsh-1*

mutants using a muscle specific promoter to express wild-type LIN-17 and DSH-1, respectively (Figure 3J and K). No rescue was observed when using a neural specific promoter (Figure S4C). In addition, receptor defects appeared specific to ACR-16::GFP, as we found no apparent change in the subcellular distribution of UNC-49::GFP or UNC-29::GFP in *cwn-2* mutants (Figure S4D).

To determine the tissue from which CWN-2 is secreted in order to mediate ACR-16/α7 localization, we used RNAi to selectively knock down expression of *cwn-2* in muscles or neurons. We found that knock down in neurons, but not in muscles, phenocopied the aberrant localization of ACR-16::GFP in *cwn-2* mutants (Figure 3L and M). Taken together, these results demonstrate the necessity of CWN-2 function in neurons, and LIN-17, CAM-1 and DSH-1 in muscles for localization of ACR-16 to the NMJ.

Wnt-signaling is required for surface expression and mobility of ACR-16/α7 at the NMJ

We hypothesized that the subsynaptic accumulation of ACR-16/α7 receptors in Wnt signaling mutants might reflect a decrease in the number of surface receptors. To test this possibility, we labeled surface ACR-16/α7 receptors by injecting fluorescently-labeled alpha-bungarotoxin (α-BgTx) into the pseudocoelomic space of transgenic wild-type and mutant worms that expressed soluble mCherry in muscle cells (Gottschalk et al., 2005; Zheng et al., 2004). In wild-type worms and Wnt signaling mutants, we observed fluorescence in muscle arms at the points of contact with the ventral cord following clearance of excess toxin by coelomocytes. This localization is consistent with a postsynaptic distribution of ACR-16/α7 receptors (Figure 4A). Because of the delay in clearing excess α-BgTx, a fraction of the fluorescence signal might also reflect internalized receptors. However, the signal was decreased in *cwn-2* and *cam-1* mutants compared to wild type suggesting that Wnt signaling promotes surface expression of ACR-16/α7 (Figure 4B). Importantly, the fluorescence signal in muscle arms was dependent on ACR-16/α7 since we did not measure appreciable α-BgTx fluorescence at muscle arms of *acr-16* mutants (Figure 4A and B). We also observed fluorescence in unidentified processes that lacked muscle mCherry expression in all of the worm strains (Figure 4A), suggesting that α-BgTx binds to additional AChRs that are expressed in neurons. This binding was unrelated to Wnt signaling or ACR-16 and served as a useful control for α-BgTx labeling.

Our results suggest that the subsynaptic accumulation of ACR-16::GFP in Wnt-signaling mutants is secondary to reduced surface expression. The percentage reduction in surface expression was roughly equivalent to the percentage reduction in ACh- and nicotine-gated currents (Figure 1E and F; Figure S2A) and provides a mechanistic explanation for the selective decrease in the fast component of ACh-gated current found in Wnt-signaling mutants.

Loss of Wnt-signaling results in decreased surface expression of ACR-16/α7 and its intracellular accumulation in muscle arms. Thus, we reasoned that Wnt-signaling might be required for delivery of ACR-16/α7 receptors from subsynaptic pools to the cell surface of the NMJ. We tested this hypothesis by using ACR-16/α7 fused to the photoconvertible fluorophore EosFP (ACR-16::EosFP) and performed optical pulse labeling experiments (Wiedenmann et al., 2004). The fluorescent signal at the distal tips of muscle arms was converted from green to red with a 405 nm laser (Figure 4C and D). We found that the red fluorescence decayed such that little signal remained in wild-type worms one hour after photoconversion (Figure 4D and E). In contrast, the decay was significantly slower in *lin-17* mutants. We also attempted to photoconvert the “neck” of the muscle arm and track the movement into the synaptic region. These experiments were technically difficult; however in the few instances that we were successful, we found reduced mobility in *lin-17* mutants (Figures S5A). These results suggest that the turnover of the subsynaptic pool of ACR-16 is

decreased in *lin-17* mutants. In addition, the longer lifetime of converted EosFP also argues against a model in which the decreased level of staining by α-BgTx in *cwn-2* and *cam-1* mutants is due to endocytosis of ACR-16/α7 followed by its rapid degradation. Together, these experiments indicate that Wnt signaling is required for the translocation of ACR-16/α7 receptors from subsynaptic pools to the NMJ and that reduced Wnt signaling leads to a large immobile pool of subsynaptic ACR-16/α7.

ACR-16/α7 is required in the adult nervous system

AChRs are critically important for synaptic function; but do they also have essential developmental roles? It is possible that the synaptic defects observed in adult *acr-16* mutants are secondary to developmental defects. For example, the molecular machinery required for postsynaptic function might not be properly assembled or stabilized in *acr-16* mutants causing irreversible changes in synaptic communication. To test whether ACR-16/α7 has an obligate developmental role, we generated *unc-29; acr-16* transgenic mutants that expressed ACR-16/α7 under an inducible heat-shock promoter (*Phsp*::*acr-16*). We heat shocked young adult transgenic worms and assayed behavior approximately 10 hours later. We found that the defective locomotion and thrashing that is characteristic of *unc-29; acr-16* double mutants were rescued in heat shocked adult transgenic mutants (Figure S5B). Furthermore, we found that heat shock rescued nicotine-gated currents (Figure S5C and D). Thus, synaptic function and behavior mediated by ACR-16/α7 could be restored in adult *unc-29; acr-16* mutants, indicating that ACR-16/α7 does not have an obligate developmental role.

Wnt signaling has an ongoing role in regulating ACR-16/α7-mediated behavior and synaptic plasticity

The Wnt signaling pathway is best known for its many developmental roles (van Amerongen and Nusse, 2009). To determine whether Wnt regulation of ACR-16/α7 at the NMJ is primarily developmental, we used a heat shock-inducible promoter to drive the expression of LIN-17 (*Phsp*::*lin-17*) in transgenic *lin-17; unc-29* double mutants. We found that normal motor behavior was restored approximately 10 hours following heat shock, but not in mutants lacking the transgene (Figure 5A). However, the rescue did not persist and thrashing rates returned to approximately pre-heat-shock levels within 24 hours, suggesting that ongoing expression of LIN-17 in adult worms is required for Wnt signaling and ACR-16/α7 dependent behavior. In addition, we observed that ACR-16::GFP fluorescence intensity in muscle arms could be rescued as early as 2 hours after heat shock driven expression of LIN-17 in adult *lin-17* mutants (Figure 5B and C). As we found for locomotion, the rescue was transient with ACR-16::GFP intensity increasing to mutant levels within 24 hours post heat shock. Together, our results suggest that Wnt signaling has an ongoing role in the maintenance of synaptic transmission in the adult nervous system.

An ongoing role for Wnt signaling suggests that ACR-16 translocation might be dynamically regulated in an experience dependent fashion. To address whether Wnt signaling contributes to experience-dependent plasticity, we expressed ChR2 in cholinergic motor neurons. We stimulated worms with light pulses to depolarize the motor neurons and measured ACR-16::GFP fluorescence in muscle arms. We found that 30 or 60 minutes of light stimulation reduced ACR-16::GFP fluorescence in wild-type worms, but not in control worms or in *cwn-2* mutants (Figure 6A and B).

We next asked whether optogenetic stimulation altered ACh-gated current at the NMJ. We found that the ACR-16-mediated current, but not the UNC-29-dependent component, was increased in worms after one hour of light stimulation; however, no stimulation-dependent increase was observed in control worms (Figure 6C and D). The decreased fluorescent signal following stimulation suggests that ACR-16::GFP is more diffuse following

translocation to the cell surface. Significantly, we did not observe a stimulation-induced augmentation of current in *cwn-2* mutants. The changes were specific to ACh-gated currents since we did not observe activity-dependent changes in GABA-activated current (Figure S6A). We also found that prolonged light stimulation increased the amplitude of both endogenous synaptic events (Figure S6B) and nerve evoked currents (Figure S6C) in wild-type worms. These activity dependent changes were dependent on neuronal expression of CWN-2. Thus, activity dependent changes were rescued in transgenic *cwn-2* mutants that expressed neuronal, but not muscle, *cwn-2* (Figure 6E and F). Furthermore, activity dependent changes were blocked by RNAi knock down of *cwn-2* in neurons, but not by knock down in muscles (Figure 6G and H). In agreement with the requirement for *cwn-2* signaling, we found that activity dependent changes were blocked in *lin-17* mutants and could be rescued in transgenic *lin-17* mutants with muscle-specific expression of a wild-type *lin-17* transgene (Figure S6D).

Wnt-mediated changes in ACR-16/α7 surface expression are independent of protein synthesis

Wnts can signal through multiple pathways, including the well-characterized canonical Wnt-signaling pathway, which depends on TCF/LEF transcription factors and new protein synthesis, and through non-canonical pathways (Korkut and Budnik, 2009; van Amerongen and Nusse, 2009). In *C. elegans, pop-1* encodes the only known TCF/LEF homologue, and we did not observe altered ACR-16::GFP following knock down of *pop-1* using RNAi (data not shown). To rigorously test the requirement for new protein synthesis in CWN-2 signaling, we adapted an existing protocol to block protein synthesis using the drug cycloheximide (CHX) (Kourtis and Tavernarakis, 2009). We found that CHX blocked new protein synthesis (Figure S7A and B), but did not have significant effects on activity-dependent changes in ACR-16::GFP (Figure 7A and B).

The neuronal requirement for Wnt-mediated changes in ACR-16/α7 translocation predicts that prolonged light-stimulation should be associated with neuronal release of CWN-2. To test this prediction, we co-expressed CWN-2::GFP and ChR2 in cholinergic motor neurons and used our light stimulation protocol to depolarize the motor neurons. We found that CWN-2::GFP fluorescence was decreased in motor neurons following light stimulation, but unchanged in control worms (Figure 7C and D). This result is consistent with activity-dependent secretion of CWN-2, but could also represent activity-dependent degradation of CWN-2. To distinguish between these possibilities, we evaluated changes in CWN-2 in the *mig-14* mutant background. The secretion of all Wnts is believed to be dependent on the Wntless transmembrane protein (Port and Basler, 2010), which is encoded by *mig-14* in *C. elegans*. We found that the activity-dependent decrease in CWN-2::GFP fluorescence was blocked in *mig-14* mutants (Figure 7C and D). This result indicates that the decrease in CWN-2::GFP in light-stimulated motor neurons is a consequence of activity-dependent secretion of CWN-2. Moreover, we selectively knocked down expression of MIG-14 in muscles or neurons and found that MIG-14 is required in neurons for ACR-16::GFP localization (Figure S7C).

Our data strongly suggest a model where neuronal activity leads to secretion of CWN-2, which then rapidly, and independently of new protein synthesis, increases ACh-gated current by mediating the translocation of additional ACR-16/α7 receptors to the muscle surface. To directly test this model, we produced recombinant CWN-2 by expressing *cwn-2* in cultured mammalian HEK cells using a previously published protocol (Cuitino et al., 2010). We found that application of recombinant CWN-2 to our dissected neuromuscular preparation rapidly (within approximately 15 minutes) caused an increase in ACh-gated current (Figure 7E and F). This result clearly shows that there is no developmental requirement for CWN-2 with respect to ACR-16/α7 translocation and that CWN-2 alone is

capable of triggering a rapid increase in the number of functional ACR-16/α7 receptors at the NMJ. Thus, we have found that the cholinergic synapse is plastic and responds by modifying surface ACR-16/α7 receptors in response to prolonged stimulation of motor neurons. These plastic changes are dependent on activity-mediated and Wntless/MIG-14-dependent secretion of CWN-2 from neurons, heteromeric CAM-1/LIN-17 postsynaptic receptors in muscle cells and the critical downstream signaling protein Dishevelled/DSH-1.

Discussion

Neuronal signaling is shaped by the time-dependent sum of the excitatory and inhibitory synaptic inputs. In *C. elegans*, the same mechanisms can be found at the NMJ, an experimentally accessible synapse ideal for mechanistic studies of synaptic function. We found that in *C. elegans*, the N-AChR ACR-16/α7-mediated currents are selectively diminished in mutants with disrupted Wnt signaling. In Wnt mutants the neuromuscular architecture is grossly normal and synaptic functions mediated by both GABAergic inputs and postsynaptic L-AChRs are indistinguishable from those in wild type. The ACR-16/α7-mediated current shares a similar dependence on the CWN-2 Wnt ligand, the CAM-1/RTK and LIN-17/Frizzled membrane proteins, and the DSH-1/dishevelled downstream effector protein. These results suggest that CAM-1 and LIN-17 contribute to a heteromeric receptor for the CWN-2 ligand; a hypothesis supported by our studies using bifluorescence complementation to map LIN-17 and CAM-1 proximity (Figure 3). Furthermore, CAM-1 and other Ror RTKs contain extracellular cysteine-rich domains that are also found in Frizzled proteins. In mammalian Ror RTKs, these domains bind Wnt5, the mammalian homologue of CWN-2 (Mikels and Nusse, 2006; Oishi et al., 2003).

In a recent study, CAM-1 appeared to associate with the Frizzled protein MIG-1 and bind to CWN-2 (Kennerdell et al., 2009). We found that a truncated variant of CAM-1 that lacks the cytoplasmic kinase domain restores ACR-16/α7-mediated current in transgenic *cam-1* mutants. This result, together with the interaction between LIN-17 and CAM-1, indicates that CAM-1/RTK contributes to CWN-2/Wnt signaling, but that the intracellular signaling is mediated primarily by LIN-17 (and DSH-1/Dvl). Thus, CAM-1 might have a direct role in regulating CWN-2 binding, or an indirect role by localizing or stabilizing LIN-17. In contrast to previously described developmental roles for CAM-1 and Wnt signaling (Green et al., 2008; van Amerongen and Nusse, 2009), we show that this signaling pathway has an ongoing functional role in regulating the strength of synaptic transmission in adult worms.

The possible contributions of Wnt signaling to the function of the adult nervous system are difficult to study and are not well understood. We found that heat-shock promoter driven expression of LIN-17 in adult *lin-17* transgenic mutants rescued ACR-16/α7-mediated behavior and ACR-16/α7 localization (Figure 5). The rescue of behavior and localization was transient, indicating rapid turnover of LIN-17 and ongoing dependence on this signaling pathway.

In support of our model that a heteromeric CAM-1/LIN-17 receptor mediates the surface expression of ACR-16/α7 in postsynaptic muscle, we found that CAM-1 and LIN-17 co-localize at the NMJ and that muscle-specific expression of CAM-1 and LIN-17 in transgenic mutants rescues ACR-16/α7-mediated current and behavior, whereas CWN-2 and MIG-14 are required in neurons. CWN-2 signaling rapidly causes translocation of ACR-16/α7 from subsynaptic pools to the cell surface, as evidenced by our finding of increased ACh-gated currents following application of recombinant CWN-2. Our data favor a model in which the levels of CWN-2 are limiting for receptor translocation and are controlled in part by neural activity. In support of this model, we found that neuronal CWN-2 levels are altered by optogenetic stimulation of the neurons, suggesting that CWN-2 secretion responds to

neuronal activity. Less clear is whether LIN-17 and CAM-1 function as constitutive heteromers; whether CWN-2 induces dimerization; or whether dimerization itself might be altered by synaptic activity. A dimerization model was proposed for CWN-2 regulation of axonal guidance (Kennerdell et al., 2009).

Heteromeric RTK/Frizzled complexes have been described for Wnt signaling during development (Lu et al., 2004; Minami et al., 2010). However, to our knowledge, a heteromeric CAM-1/LIN-17 receptor complex participating in Wnt-mediated signaling at adult synapses has not been previously described, and contrasts with the known signaling roles for CAM-1 and LIN-17. Presumably, the heteromeric complex provides additional signaling specificity, e.g., shunting signaling from the canonical pathway to an alternate pathway, such as the PCP pathway, to cause rapid changes in receptor translocation and synaptic transmission.

Dynamic translocation of receptors from subcellular pools to the surface membrane is an essential and conserved feature found in diverse signaling pathways. Yet we still lack a comprehensive understanding of how extracellular signals lead to precise translocation of receptors. Our data suggest that Wnt signaling regulates the translocation of subsynaptic ACR-16/α7 receptors to muscle arm synapses in *C. elegans*. Thus, in Wnt-signaling mutants ACR-16/α7 receptors accumulate in subsynaptic pools and surface expression is reduced. Associated with decreased surface expression of ACR-16/α7 is a marked reduction in receptor mobility as defined by photoconversion experiments (Figure 4). Interestingly, CWN-2/Wnt signaling does not appear to have an effect on GABARs, L-AChRs or the currents mediated by these receptors. Thus, we were able to cleanly dissect and distinguish the signaling pathway that contributes to ACR-16/α7 synaptic signaling from other developmental or regulatory pathways.

We also found that cholinergic synapses at the NMJ are plastic and their strength is modified by prolonged activity. Under our conditions of optogenetic stimulation, ACR-16/α7 puncta diminished in size and ACh-gated current was increased. These effects were not observed in *cwn-2* mutants. Perhaps different environmental challenges, e.g., increased load or resistance, are associated with increased nervous system activity, which then leads to a Wnt-mediated recruitment of additional receptors. We envision a model where synaptic strength is dynamically modulated by translocation of receptors regulated by a Wnt signaling pathway. This mode of regulation might be evolutionarily conserved and could contribute to fundamental processes of synaptic plasticity and homeostasis in other organisms and for other classes of synaptic receptors.

Experimental Procedures

Strains, Genetics, and Germline Transformation

All *C. elegans* strains were raised under standard conditions on the *E. coli* strain OP50 at 20° C unless otherwise noted (Brenner, 1974). Wild-type worms were the Bristol N2 strain. Mutant alleles used were *cam-1(ak37)*, *cwn-2(ok895)*, *lin-17(n671)*, *dsh-1(ok1445)*, *acr-16(ok789)*, *unc-29(x29)*, *cwn-1(ok546)*, *cfz-2(ok1201)*, *egl-20(n585ts)*, *lin-44(n1792)*, *mig-1(e1787)*, *mig-14(mu71)*, and *lin-18(e620)*. Plasmids, transgenic arrays and strains are described in Supplemental Experimental Procedures. All fluorescently labeled proteins were found to be functional in transgenic rescue experiments of the respective mutant phenotype.

Behavioral Analysis

Thrashing assays were performed as described previously (Francis et al., 2005). All thrashing assays were done blind. For heat-shock rescue experiments, worms were kept at 30° C for 30 min. For movement on agarose, worms were mounted on 5% agarose pads with

1 μl of Polybead Microspheres 0.625% (w/v) in M9 solution and covered with a glass cover slip (Fang-Yen, et al., Worm Breeders Gazette, Vol. 18, 2010). Time-lapse images were acquired for 30 s with a Hamamatsu CCD camera using a 10× 0.5 NA Zeiss objective mounted on an inverted Zeiss compound microscope. Images were acquired with Metamorph software and analyzed with ImageJ software. Statistical significance was determined using Student's T-test.

Electrophysiological analysis

Ligand-gated currents were recorded from voltage-clamped muscle cells using patch-clamp technology as previously described (Francis et al., 2005). Drugs were applied for 250 ms using pressure application. All drugs were used at a concentration of 100 μM. Light-evoked currents were elicited from worms expressing ChR2 under the *unc-17* promoter following a recently described protocol (Liu et al., 2009).

Microscopy and labeling

For confocal fluorescence microscopy, worms were mounted on agarose pads and imaged as previously described (Francis, 2005). For ACR-16::GFP intensity analysis in muscle arms, image stacks were imported into ImageJ software for maximum projection analysis. A region of interest (ROI) was drawn around individual muscle arms along the ventral nerve cord in one-day old adult worms and the average intensity was calculated with correction for background fluorescence. There was no significant difference in the ROI area (pixels) for all genotypes. For CWN-2::GFP quantification, a ROI was drawn around each motor neuron cell body and the average intensity was calculated for light (+) retinal (−) after correcting for background fluorescence. This value was then used to normalize activity-dependent changes in GFP. Surface expression of ACR-16/α7 was assessed with α-bungarotoxin conjugated to Alexa Fluor 488 (Molecular Probes). All analyses were done blind to genotype. Additional details about confocal microscopy and labeling are found in Supplemental Experimental Procedures.

EosFP photoconversion

Worms were immobilized on agarose pads (Fang-Yen, et al., Worm Breeders Gazette, Vol. 18, 2010) and single ACR-16::EosFP puncta at the tips of distinct muscle arms were converted using a single 3 s pulse of a 405 nm laser set to a total output of 35 mW applied to a Mosaic II digital mirror device (Photonics) controlled by Metamorph software. Confocal stack images were acquired before, immediately after, and at various time points after conversion as described above. The time-dependent photoconverted signal was expressed as a percentage of the signal immediately following photoconversion. For pulse-chase experiments, statistical significance was determined using a 2-way ANOVA test.

Synaptic Plasticity

Transgenic worms expressed ChR2 under control of the *unc-17* promoter, which drives expression in the cholinergic motor neurons. Worms were stimulated with 470 nm light delivered by a Lambda DG4 light source (Sutter). Light intensity at the surface of the NGM (nematode growth media) was approximately 240 $\mu W/mm^2$ and worms were stimulated at 3 Hz with 100 ms pulses of light for specified durations (Lui, 2009).

Recombinant CWN-2

We expressed *cwn-2* in mammalian HEK cells as previously described (Cuitino et al., 2010). Briefly, HEK cells were stably transfected with Lipofectamine (Invitrogen) with either empty vector pcDNA or pcDNA encoding *cwn-2* cDNA coupled to a hemagglutinin (HA) tag. HEK cell supernatant was then collected and concentrated using a Centrifugal

Filter Device (Millipore; 30 kDa), and diluted 1 to 50 in ECF (1 mM Ca^{2+}). Secreted CWN-2 was detected by western blot using a HA-specific antibody.

Supplementary Material

Refer to Web version on PubMed Central for supplementary material.

Acknowledgments

We thank members of the Maricq laboratory for comments on the manuscript, Kang Shen and Erik Jorgensen for plasmids and transgenic strains, and the *Caenorhabditis* Genetics Center [funded by the National Institutes of Health (NIH)] for providing worm strains. This research was made possible by support from NIH Grant R01 NS070280 and American Heart Association Predoctoral Grant 09PRE2060730 (MJ).

References

Ataman B, Ashley J, Gorczyca M, Ramachandran P, Fouquet W, Sigrist SJ, Budnik V. Rapid activity-dependent modifications in synaptic structure and function require bidirectional Wnt signaling. Neuron. 2008; 57:705–718. [PubMed: 18341991]

Boulin T, Gielen M, Richmond JE, Williams DC, Paoletti P, Bessereau JL. Eight genes are required for functional reconstitution of the Caenorhabditis elegans levamisole-sensitive acetylcholine receptor. Proc Natl Acad Sci U S A. 2008; 105:18590–18595. [PubMed: 19020092]

Brown D, Breton S, Ausiello DA, Marshansky V. Sensing, signaling and sorting events in kidney epithelial cell physiology. Traffic. 2009; 10:275–284. [PubMed: 19170982]

Budnik V, Salinas PC. Wnt signaling during synaptic development and plasticity. Curr Opin Neurobiol. 2011; 21:151–159. [PubMed: 21239163]

Ciani L, Boyle KA, Dickins E, Sahores M, Anane D, Lopes DM, Gibb AJ, Salinas PC. Wnt7a signaling promotes dendritic spine growth and synaptic strength through Ca(2)/Calmodulin-dependent protein kinase II. Proc Natl Acad Sci U S A. 2011; 108:10732–10737. [PubMed: 21670302]

Cuitino L, Godoy JA, Farias GG, Couve A, Bonansco C, Fuenzalida M, Inestrosa NC. Wnt-5a modulates recycling of functional GABAA receptors on hippocampal neurons. J Neurosci. 2010; 30:8411–8420. [PubMed: 20573888]

de Bono M, Maricq AV. Neuronal substrates of complex behaviors in C. elegans. Annu Rev Neurosci. 2005; 28:451–501. [PubMed: 16022603]

Farias GG, Godoy JA, Cerpa W, Varela-Nallar L, Inestrosa NC. Wnt signaling modulates pre- and postsynaptic maturation: therapeutic considerations. Dev Dyn. 2010; 239:94–101. [PubMed: 19681159]

Farias GG, Valles AS, Colombres M, Godoy JA, Toledo EM, Lukas RJ, Barrantes FJ, Inestrosa NC. Wnt-7a induces presynaptic colocalization of alpha 7-nicotinic acetylcholine receptors and adenomatous polyposis coli in hippocampal neurons. J Neurosci. 2007; 27:5313–5325. [PubMed: 17507554]

Francis MM, Evans SP, Jensen M, Madsen DM, Mancuso J, Norman KR, Maricq AV. The Ror receptor tyrosine kinase CAM-1 is required for ACR-16-mediated synaptic transmission at the C. elegans neuromuscular junction. Neuron. 2005; 46:581–594. [PubMed: 15944127]

Gleason JE, Szyleyko EA, Eisenmann DM. Multiple redundant Wnt signaling components function in two processes during C. elegans vulval development. Dev Biol. 2006; 298:442–457. [PubMed: 16930586]

Gottschalk A, Almedom RB, Schedletzky T, Anderson SD, Yates JR 3rd, Schafer WR. Identification and characterization of novel nicotinic receptor-associated proteins in Caenorhabditis elegans. Embo J. 2005; 24:2566–2578. [PubMed: 15990870]

Green JL, Inoue T, Sternberg PW. The C. elegans ROR receptor tyrosine kinase, CAM-1, non-autonomously inhibits the Wnt pathway. Development. 2007; 134:4053–4062. [PubMed: 17942487]

Green JL, Kuntz SG, Sternberg PW. Ror receptor tyrosine kinases: orphans no more. Trends Cell Biol. 2008; 18:536–544. [PubMed: 18848778]

Hall AC, Lucas FR, Salinas PC. Axonal remodeling and synaptic differentiation in the cerebellum is regulated by WNT-7a signaling. Cell. 2000; 100:525–535. [PubMed: 10721990]

Henriquez JP, Webb A, Bence M, Bildsoe H, Sahores M, Hughes SM, Salinas PC. Wnt signaling promotes AChR aggregation at the neuromuscular synapse in collaboration with agrin. Proc Natl Acad Sci U S A. 2008; 105:18812–18817. [PubMed: 19020093]

Inestrosa NC, Arenas E. Emerging roles of Wnts in the adult nervous system. Nat Rev Neurosci. 2010; 11:77–86. [PubMed: 20010950]

Jin Y, Garner CC. Molecular mechanisms of presynaptic differentiation. Annu Rev Cell Dev Biol. 2008; 24:237–262. [PubMed: 18588488]

Kennedy MJ, Ehlers MD. Mechanisms and function of dendritic exocytosis. Neuron. 2011; 69:856–875. [PubMed: 21382547]

Kennerdell JR, Fetter RD, Bargmann CI. Wnt-Ror signaling to SIA and SIB neurons directs anterior axon guidance and nerve ring placement in C. elegans. Development. 2009; 136:3801–3810. [PubMed: 19855022]

Kessels HW, Malinow R. Synaptic AMPA receptor plasticity and behavior. Neuron. 2009; 61:340–350. [PubMed: 19217372]

Kim C, Forrester WC. Functional analysis of the domains of the C elegans Ror receptor tyrosine kinase CAM-1. Dev Biol. 2003; 264:376–390. [PubMed: 14651925]

Korkut C, Ataman B, Ramachandran P, Ashley J, Barria R, Gherbesi N, Budnik V. Trans-synaptic transmission of vesicular Wnt signals through Evi/Wntless. Cell. 2009; 139:393–404. [PubMed: 19837038]

Korkut C, Budnik V. WNTs tune up the neuromuscular junction. Nat Rev Neurosci. 2009; 10:627–634. [PubMed: 19693027]

Kourtis N, Tavernarakis N. Cell-specific monitoring of protein synthesis in vivo. PLoS One. 2009; 4:e4547. [PubMed: 19234598]

Liewald JF, Brauner M, Stephens GJ, Bouhours M, Schultheis C, Zhen M, Gottschalk A. Optogenetic analysis of synaptic function. Nat Methods. 2008; 5:895–902. [PubMed: 18794862]

Liu Q, Hollopeter G, Jorgensen EM. Graded synaptic transmission at the Caenorhabditis elegans neuromuscular junction. Proc Natl Acad Sci U S A. 2009; 106:10823–10828. [PubMed: 19528650]

Lu W, Yamamoto V, Ortega B, Baltimore D. Mammalian Ryk is a Wnt coreceptor required for stimulation of neurite outgrowth. Cell. 2004; 119:97–108. [PubMed: 15454084]

Mikels AJ, Nusse R. Purified Wnt5a protein activates or inhibits beta-catenin-TCF signaling depending on receptor context. PLoS Biol. 2006; 4:e115. [PubMed: 16602827]

Minami Y, Oishi I, Endo M, Nishita M. Ror-family receptor tyrosine kinases in noncanonical Wnt signaling: their implications in developmental morphogenesis and human diseases. Dev Dyn. 2010; 239:1–15. [PubMed: 19530173]

Oishi I, Suzuki H, Onishi N, Takada R, Kani S, Ohkawara B, Koshida I, Suzuki K, Yamada G, Schwabe GC, et al. The receptor tyrosine kinase Ror2 is involved in non-canonical Wnt5a/JNK signalling pathway. Genes Cells. 2003; 8:645–654. [PubMed: 12839624]

Port F, Basler K. Wnt trafficking: new insights into Wnt maturation, secretion and spreading. Traffic. 2010; 11:1265–1271. [PubMed: 20477987]

Richmond JE, Jorgensen EM. One GABA and two acetylcholine receptors function at the C. elegans neuromuscular junction. Nat Neurosci. 1999; 2:791–797. [PubMed: 10461217]

Sahores M, Gibb A, Salinas PC. Frizzled-5, a receptor for the synaptic organizer Wnt7a, regulates activity-mediated synaptogenesis. Development. 2010; 137:2215–2225. [PubMed: 20530549]

Shyu YJ, Hiatt SM, Duren HM, Ellis RE, Kerppola TK, Hu CD. Visualization of protein interactions in living Caenorhabditis elegans using bimolecular fluorescence complementation analysis. Nat Protoc. 2008; 3:588–596. [PubMed: 18388940]

Touroutine D, Fox RM, Von Stetina SE, Burdina A, Miller DM 3rd, Richmond JE. acr-16 encodes an essential subunit of the levamisole-resistant nicotinic receptor at the Caenorhabditis elegans neuromuscular junction. J Biol Chem. 2005; 280:27013–27021. [PubMed: 15917232]

Turrigiano GG. The self-tuning neuron: synaptic scaling of excitatory synapses. Cell. 2008; 135:422–435. [PubMed: 18984155]

van Amerongen R, Nusse R. Towards an integrated view of Wnt signaling in development. Development. 2009; 136:3205–3214. [PubMed: 19736321]

Watson RT, Pessin JE. GLUT4 translocation: the last 200 nanometers. Cell Signal. 2007; 19:2209–2217. [PubMed: 17629673]

Wiedenmann J, Ivanchenko S, Oswald F, Schmitt F, Rocker C, Salih A, Spindler KD, Nienhaus GU. EosFP, a fluorescent marker protein with UV-inducible green-to-red fluorescence conversion. Proc Natl Acad Sci U S A. 2004; 101:15905–15910. [PubMed: 15505211]

Wu H, Xiong WC, Mei L. To build a synapse: signaling pathways in neuromuscular junction assembly. Development. 2010; 137:1017–1033. [PubMed: 20215342]

Zheng Y, Mellem JE, Brockie PJ, Madsen DM, Maricq AV. SOL-1 is a CUB-domain protein required for GLR-1 glutamate receptor function in C. elegans. Nature. 2004; 427:451–457. [PubMed: 14749834]

Zinovyeva AY, Yamamoto Y, Sawa H, Forrester WC. Complex network of Wnt signaling regulates neuronal migrations during Caenorhabditis elegans development. Genetics. 2008; 179:1357–1371. [PubMed: 18622031]

Highlights

- Wnt signaling by neurons in *C. elegans* regulates synaptic transmission and plasticity
- CWN-2 signals via a novel heteromeric CAM-1/Ror RTK and LIN-17/Frizzled receptor
- CWN-2 causes rapid translocation of ACR-16/α7 receptors to the postsynaptic membrane
- Heat-shock driven CWN-2 signaling in adult mutants rescues ACR-16-mediated behavior

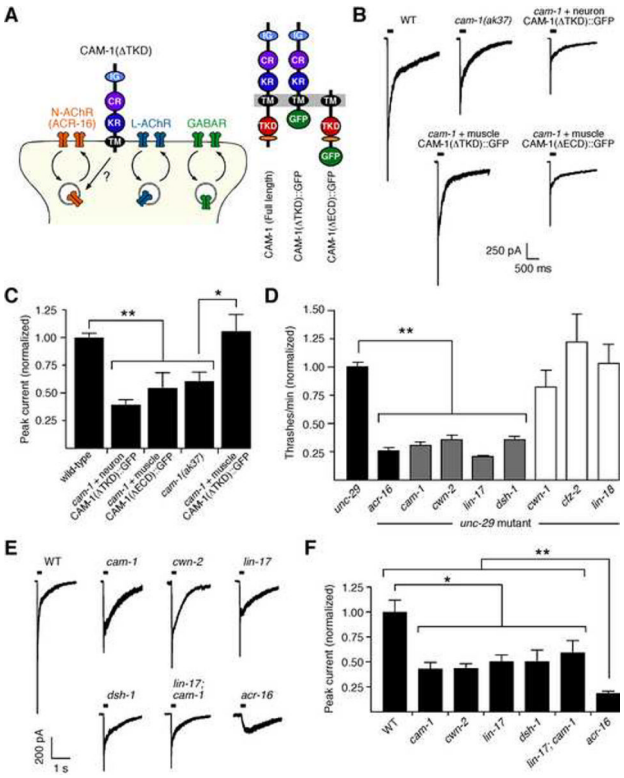

Figure 1.

Wnt and CAM-1/Ror signaling proteins contribute to synaptic signaling.

(A) Schematic of the NMJ showing the three classes of ligand-gated receptors and deletion variants of the CAM-1/Ror RTK. The orange oblong represents the serine/threonine rich domain. (B) Currents recorded in muscle cells in response to pressure application of 100 uM ACh in wild-type worms, *cam-1(ak37)* mutants, and transgenic mutants that expressed either CAM-1(ΔECD)::GFP or CAM-1(ΔTKD)::GFP in muscles or neurons, respectively. (C) Normalized peak ACh-gated current, n≥4 for all genotypes. (D) Thrashing behavior of Wnt-signaling mutants in the *unc-29(x29)* mutant background. For all genotypes, n≥10. (E) ACh-gated currents in the muscle cells of wild-type (WT) and mutant worms. (F) Peak ACh-gated current normalized to wild-type values. For all genotypes, n≥5. *, $p<0.05$; **, $p<0.01$. Error bars indicate SEM. See also Figure S1, S2 and S3.

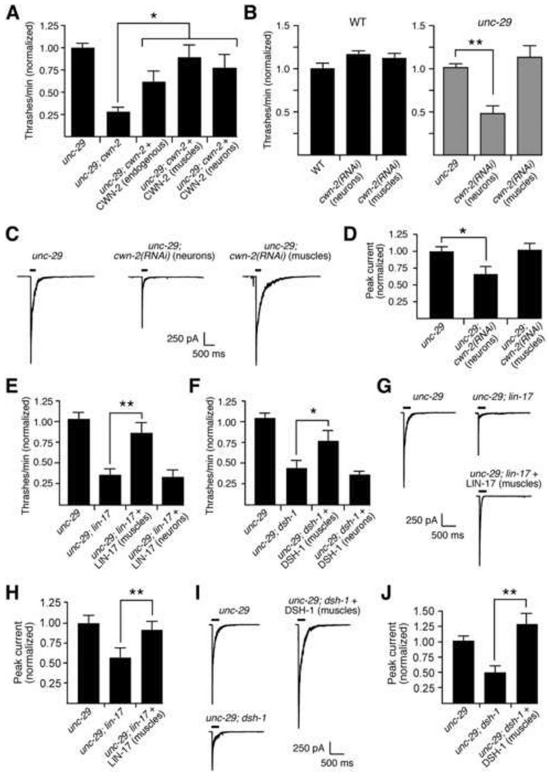

Figure 2.

ACR-16/α7-dependent behavior requires neuronal CWN-2 and Fzd/Ror/Dvl in muscles. (A) Thrashing behavior normalized to *unc-29* single mutants. For all genotypes, n≥7. (B) Thrashing behavior normalized to wild-type (WT) worms (left) or *unc-29* mutants (right) in transgenic worms in which *cwn-2* was knocked down [*cwn-2(RNAi)*] in either neurons or muscles. For WT background, n≥5; and *unc-29* mutant background, n≥10. Gray bars indicate *unc-29* mutant background. (C) ACh-gated currents in *unc-29* mutants with or without *cwn-2* knock down. (D) Peak ACh-gated current normalized to *unc-29* mutants. For all genotypes, n≥4. (E and F) Thrashing behavior showing muscle specific rescue of *lin-17* (E) and *dsh-1* (F) mutants. For all genotypes, n≥9. (G and I) Currents evoked in muscle cells by pressure application of 100 μM ACh. (H and J) Average peak current amplitude of ACh-gated currents. For all genotypes, n≥4. *, $p<0.05$; **, $p<0.01$. Error bars indicate SEM. See also Figure S3.

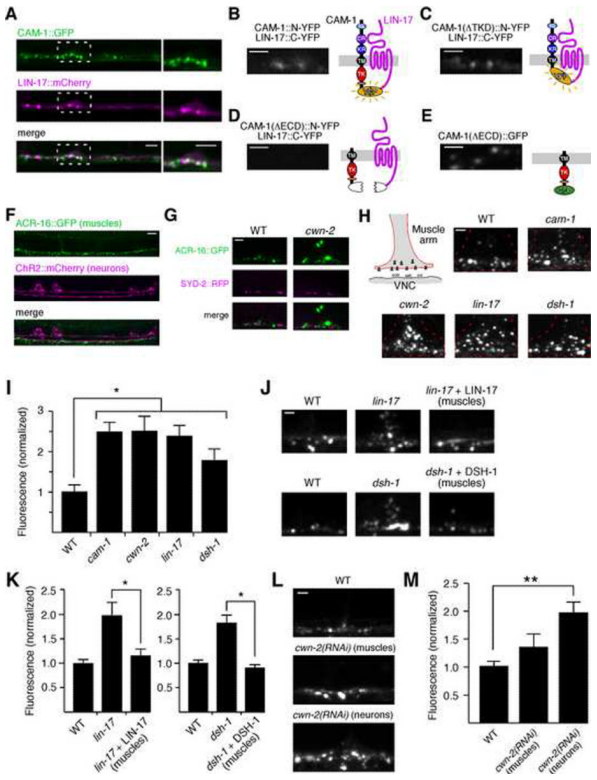

Figure 3.

Muscle LIN-17/CAM-1 heteromeric receptors regulate ACR-16 localization.

(A) Single plane confocal images showing expression of CAM-1::GFP and LIN-17::mCherry in the tips of muscle arms. Box indicates the region shown in the images on the right. Scale bars, 2 μm. (B–E) Images of the tips of muscle arms in transgenic worms that expressed split-YFP fused to LIN-17 and either full-length CAM-1 (B), one of two CAM-1 deletion variants (C and D), or CAM-1(ΔECD)::GFP (E). Scale bars, 1 μm. (F) Image of the ventral nerve chord in a transgenic worm that expressed ACR-16::GFP in muscle cells and ChR2::mCherry in motor neurons. Scale bar, 5 μm. (G) ACR-16::GFP and SYD-R::RFP expression in the muscle arm of a transgenic wild-type (WT) worm or *cwn-2* mutant. Scale bar, 2 μm. (H) Images of muscle arms in transgenic wild-type and mutant worms that expressed ACR-16::GFP. The red, dashed lines outline the muscle arms. Scale bar, 1 μm. (I) Intensity of ACR-16::GFP fluorescence in muscle arms normalized to wild type. For all genotypes, n≥8. (J) Images of ACR-16::GFP expression in muscle arms. Scale bar, 1 μm. (K) Intensity of ACR-16::GFP fluorescence in muscle arms relative to wild-type. For all genotypes, n≥11. (L) ACR-16::GFP expression in muscle arms of wild-type worms with or without *cwn-2* knock down. Scale bar, 2 μm. (M) ACR-16::GFP fluorescence intensity in muscle arms relative to wild type, n≥11. *, p<0.05; **, p<0.01. Error bars indicate SEM. See also Figure S4.

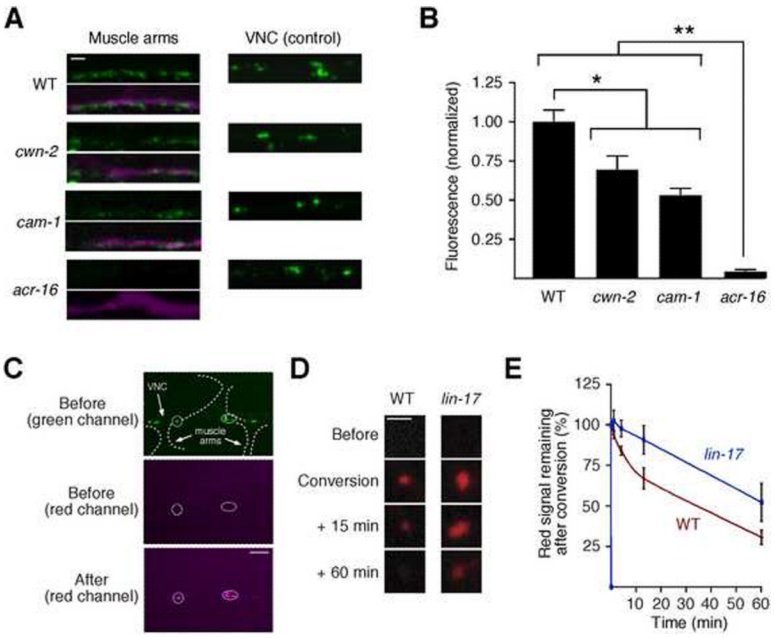

Figure 4.

ACR-16::GFP is mislocalized and its mobility reduced in Wnt-signaling mutants.

(A) Images of the tips of muscle arms in transgenic wild-type (WT) and mutant worms injected with fluorescently labeled α-BgTx. These worms also expressed soluble mCherry in muscle cells to identify muscle arms. Scale bar, 1 μm. (B) Quantification of α-BgTx fluorescence. *, $p<0.05$; **, $p<0.01$. For all genotypes, $n\geq12$. (C) Images of muscle arms in a wild-type transgenic worm that expressed ACR-16::EosFP both before and after photoconversion from green to red. The white, dashed lines outline individual muscle arms. The circles show the converted EosFP puncta. Scale bar, 5 μm. (D) Loss of fluorescence observed with photoconversion-chase strategy. Shown are examples of the loss of ACR-16::EosFP fluorescence in muscle arms following photoconversion from green to red. Scale bar, 1 μm. (E) Quantification of EosFP after photoconversion in wild-type worms and *lin-17* mutants ($n\geq11$). *lin-17* mutants are significantly different from WT, $p<0.001$. Error bars represent SEM. See also Figure S5.

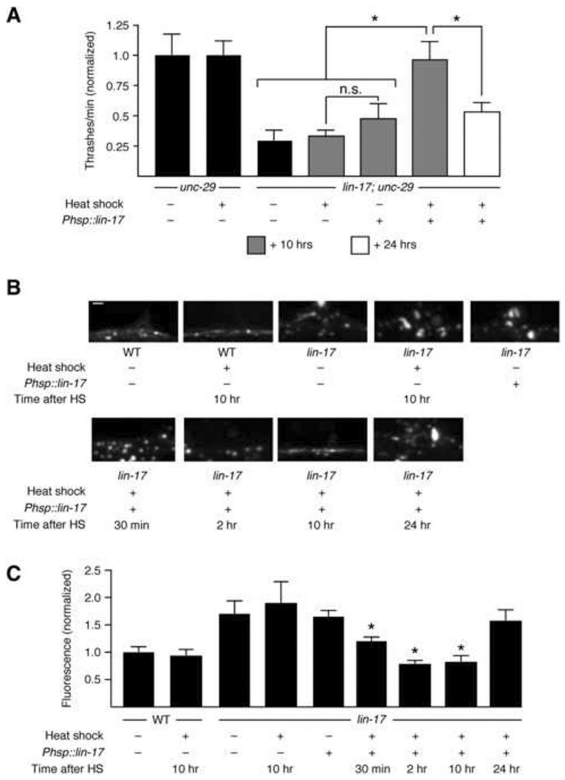

Figure 5.

LIN-17 expression in adult mutants rescues ACR-16-mediated behavior and receptor localization.

(A) Thrashing behavior in *unc-29* single mutants, *lin-17; unc-29* double mutants and transgenic double mutants that expressed *Phsp::lin-17*. n≥10 for each strain and condition. Shown is behavior 10 and 24 hrs following heat shock. (B) Images of ACR-16::GFP expression in the muscle arms of wild-type (WT) worms, *lin-17* mutants and transgenic mutants following heat shock (HS). Scale bar, 1 μm. (C) Intensity of ACR-16::GFP fluorescence relative to wild-type worms. n≥9 for each strain and condition. *, significantly different from *lin-17*, heat shock (−), $p<0.05$. Error bars indicate SEM. See also Figure S5.

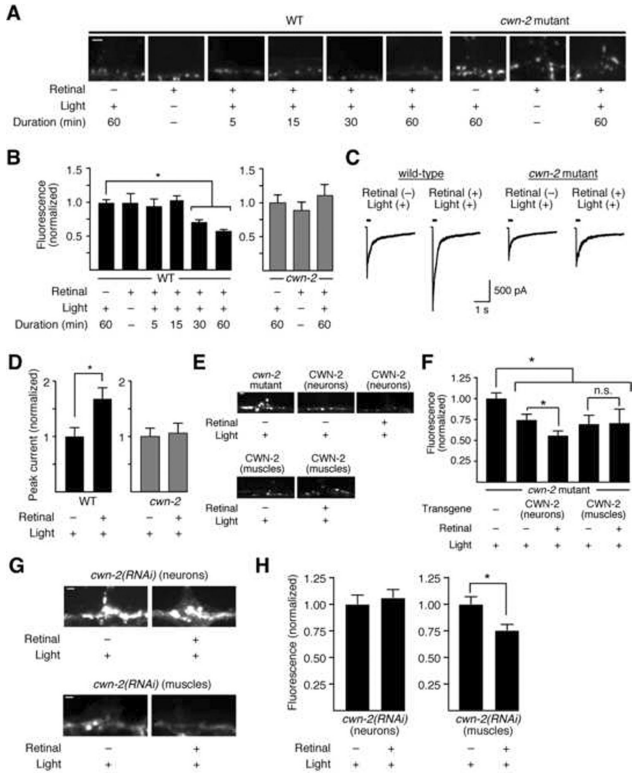

Figure 6.

Chronic stimulation of the NMJ modifies ACR-16 localization and ACh-gated current. (A) ACR-16::GFP in muscle arms of transgenic wild type (WT) and *cwn-2* mutant worms that expressed ChR2 with or without light stimulation and in the presence or absence of retinal. Scale bar, 1 μm. (B) Quantification of GFP fluorescence in the worms shown in (A). Normalized to WT, retinal (−) (black bars) or *cwn-2*, retinal (−) (gray bars). For all strains and conditions, n≥12. (C) ACh-gated currents in the muscle cells of light stimulated, transgenic worms that expressed ChR2 in motor neurons. (D) Peak ACh-gated current amplitude normalized to WT, retinal (−) (black bars) or *cwn-2*, retinal (−) (gray bars). For each genotype and condition, n≥6. *, $p<0.05$. (E) ACR-16::GFP expression in muscle arms of *cwn-2* mutants with or without a wild-type *cwn-2* transgene expressed in muscles or neurons. Scale bar, 2 μm. (F) Quantification of ACR-16::GFP fluorescence normalized to transgene (−) controls. For all genotypes and conditions, n≥18. (G) ACR-16::GFP fluorescence in muscle arms of light-stimulated, transgenic wild-type worms with *cwn-2* knock down in either muscles or neurons. Scale bar, 1 μm. (H) Quantification of ACR-16::GFP fluorescence in muscle arms. For all genotypes and conditions, n≥15. *, $p<0.05$. Error bars indicate SEM. See also Figure S6.

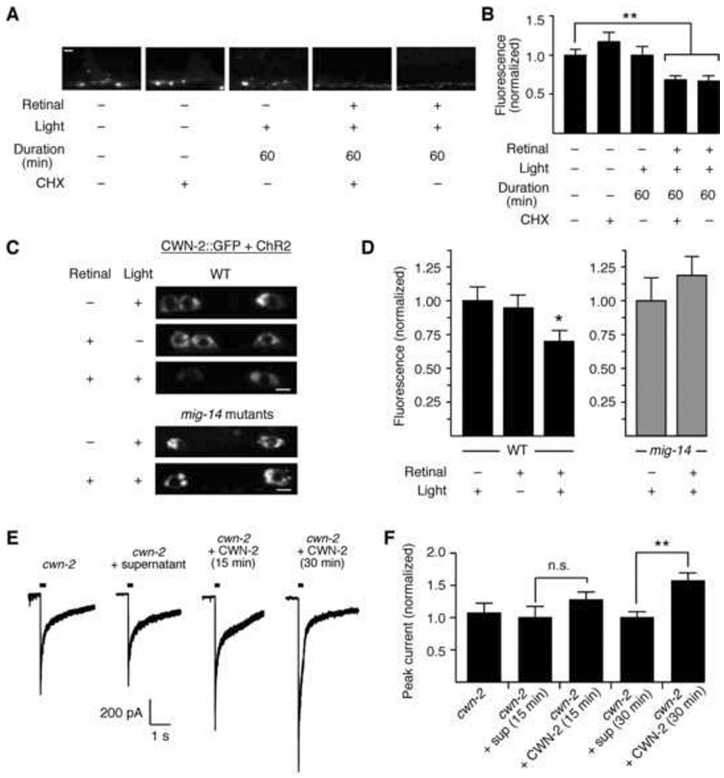

Figure 7.

Translocation of ACR-16/α7 is independent of protein synthesis and rapidly induced by recombinant CWN-2.

(A) ACR-16::GFP expression in muscle arms of transgenic wild-type worms that expressed ChR2 in motor neurons. Scale bar, 2 μm. (B) Quantification of ACR-16::GFP fluorescence intensity normalized to retinal (−), light (−), CHX (−) control. For all conditions, n≥9. (C) CWN-2::GFP expression in motor neuron cell bodies in transgenic wild-type (WT) and *mig-14* mutant worms. Scale bars, 4 μm. (D) Quantification of CWN-2::GFP fluorescence intensity normalized to either WT, retinal (−) (black bars) or *mig-14*, retinal (−) (gray bars). For all genotypes and conditions, n≥16. (E) ACh-gated currents in *cwn-2* mutants with or without the application of recombinant CWN-2. (F) Quantification of peak ACh-gated current normalized to *cwn-2* control. For all conditions, n≥4. *,p<0.05, **p<0.01. Error bars indicate SEM. See also Figure S7.